Neutron measurements at the ELISE neutral beam test facility and implications for neutron based diagnostics at SPIDER[a)]

S. Feng,[1, b)] M. Nocente,[1, 2, c)] D. Wünderlich,[3] F. Bonomo,[3] G. Croci,[1, 2] U. Fantz,[3] B. Heinemann,[3] W. Kraus,[3] I. Mario,[3] A. Muraro,[2] R. Pasqualotto,[4] M. Rebai,[2] M. Tardocchi,[2] and G. Gorini[1, 2]

[1)] *Dipartimento di Fisica "G. Occhialini", Università di Milano-Bicocca, Milano, Italy*

[2)] *Istituto di Fisica del Plasma "P. Caldirola", Consiglio Nazionale delle Ricerche, Milano, Italy*

[3)] *Max Planck Institut für Plasmaphysik, Garching, Germany*

[4)] *Consorzio RFX, Padova, Italy*

(Dated: 2 July 2018)

Along the route to the development of a neutral beam injector for ITER, the Padua based SPIDER and MITICA facilities will make use of neutron diagnostics to quantify the homogeneity of the neutral beam profile by measuring the map of the neutron emission from the beam dump with the close-contact neutron emission surface mapping (CNESM) system. Neutrons are here produced from beam-target reactions between the deuterium beam and the deuterons previously adsorbed in the calorimeter. In order to aid the interpretation of the diagnostic data, a dedicated experiment on neutron emission from beam-target reactions with beam parameters approaching those expected at SPIDER has been performed at the ELISE neutral beam test facility. The time trace of neutron emission has been measured using a calibrated liquid scintillator detector at increasing power densities on the target. Compared to calculations based on the local mixing model, a systematic discrepancy was observed exceeding the statistical accuracy of the measurements and increasing as a linear function of the power density. The data are used to derive an empirical temperature dependent correction for applications to neutron measurements at SPIDER.

I. INTRODUCTION

The PRIMA (Padova Research on ITER Megavolt Accelerator) neutral beam test facility which is designed to demonstrate the feasibility of a prototype neutral beam injector for ITER is under construction in Padova, Italy[1,2]. PRIMA includes the negative ion source SPIDER (Source for Production of Ion of Deuterium Extracted from Rf plasma) and the full power injector MITICA (Megavolt ITER Injector & Concept Advancement). SPIDER is the necessary step before MITICA because it has to demonstrate extraction and acceleration to 100 keV of a large negative ion hydrogen or deuterium beam with uniform intensity and low divergence. In order to well estimate the beam uniformity and divergence, a set of diagnostics including the CNESM (close-contact neutron emission surface mapping) system have been designed[3]. CNESM system is based on Gas Electron Multiplier (GEM) detectors for neutron detection with the aim to resolve the 2D beam intensity profile in deuterium operations at SPIDER[4–7]. Here, fusion reactions between beam deuterons and deuterons implanted in the copper beam dump will produce about 10^{12} neutrons/s spread over 1 m^2. Then the footprint of the deuterium beam that hits the dump can be retrieved from the spatial map of the neutron emission intensity obtained by the CNESM[8–10]. In SPIDER, CNESM will be benchmarked by STRIKE, an inertially cooled calorimeter as the main diagnostics for the beam profile mainly based on Infra-red (IR) measurements. As IR measurements cannot be used on MITICA due to engineering constraints, the experience gained at SPIDER will be instrumental to make CNESM the reference system for deuterium beam profile measurements on MITICA[11]. In order to aid the detector development, neutron emission from $D(d,n)^3He$ reactions in the beam target experiment must be investigated first.

A parasitic experiment was first performed at the ELISE facility[12]. The time evolution of beam-target neutron emission from the dump was measured by using a calibrated EJ301 liquid scintillator and has been compared with calculations based on the Local Mixing Model (LMM)[13,14] on a relative scale. Calculations could reproduce the general qualitative features of the measured time trace of neutron emission but, at a more quantitative level, overestimated the neutron emission up to 30%, which could be due to systematic uncertainties of the input data. Benefiting from later refinements of the method to analyse data from the diagnostic calorimeter[11], a moderate discrepancy up to 12% between the LMM based calculation and data in the power range 160 kW to 440 kW has been revealed in a new experiment[15]. This, if extrapolated to SPIDER, would imply a deficit as large as 70% in full power deuterium operations. On the other hand, the power density on the dump at SPIDER will be a factor four larger than the values tested at ELISE in our previous experiment[15] and a linear, empirical extrapolation of our results to SPIDER might be questionable.

To the purpose of verifying whether the deficit still ex-

[a)] Contributed paper published as part of the Proceedings of the 22nd Topical Conference on High-Temperature Plasma Diagnostics, San Diego, California, April, 2018.

[b)] Electronic mail: f.song@campus.unimib.it

[c)] Electronic mail: massimo.nocente@mib.infn.it

trapolates linearly towards the beam power expected at SPIDER, we have performed a dedicated experiment that explores a parameter range approaching the maximum capabilities allowed by the ELISE facility[16] of the Max Planck Institut für Plasmaphysik (IPP) (Garching, Germany), where the beam power was scanned from about 200 kW to 950 kW by modifying the beam current and/or voltage in a controlled manner. Particular attention was paid to ensuring a constant beam size and profile as the power was scanned. A neutron detector was used to monitor the time trace of neutron emission and the result has been compared with LMM based calculations on a relative scale (see below). The results are also used to determine an empirical correction for CNESM applications at SPIDER.

II. BEAM-TARGET NEUTRON EMISSION EXPERIMENT

A. Operation of pulsed deuterium beams

ELISE is a half size ITER NBI test facility which can produce a negative ion beam up to 60 keV for 10 seconds (s) every 3 minutes[17,18]. The experiment here described is based on 231 deuterium pulses in 3 different experimental days. For each pulse, we measured the time trace of the neutron emission as a function of time with the calibrated liquid scintillator described below. The filling pressure was set to 0.6 Pa and the operation parameters including the average beam currents, high voltages (HV) and power on the dump in the experiment are shown in table I. For pulses marked by an asterisk the power on the dump was gradually increased up to the target value. For those pulses, the starting value of the power, HV and current used are also indicated within parentheses. The highest beam power deposited on the dump was achieved at about 950 kW.

TABLE I: Operation parameters of the deuterium beam in the neutron emission experiment.

Nr. pulses	Power(kW)	HV(keV)	Current(A)
4	190	30.1	6.3
20	214	30.1	7.1
22	304	30.1	10.1
21	397	35.1	11.3
21	500	37.6	13.3
23	605	42	14.4
16*	683 (160)	46.5 (30.1)	14.7 (5.3)
22	706	47.1	15
28	784	49.3	15.9
8*	592 (210)	44.5 (35)	13.3 (6.0)
21	655	45.5	14.4
25	898	54.1	16.6

A copper calorimeter (with a total surface of 1.2 m × 1.2 m) consists of 30 × 30 blocks[11] and is placed at a distance of 3.5 m from the extraction and acceleration system[19] to stop the beam. Each block is made of pure copper (38 × 38 × 25 mm) and can be considered as an inertial dump. It is cooled down in the time interval between two consecutive pulses by the cooling system on the rear side of the blocks. The side facing the beam is coated with Molybdenum Disulfide (MoS_2) to perform IR analysis. This is done by a FLIR A655sc IR micro-bolometer camera which is triggered five seconds before the HV phase and acquires IR images for one minute, including the 10 s beam time. Thermocouples installed in 48 copper blocks of the calorimeter make it possible to calibrate the camera on an absolute scale. From the power deposition on the calorimeter surface one can then determine a 2D profile of the beam current on the dump, as well as the beam size and uniformity for later use in the calculations (see section III). A 2D beam power map (profile) at low (300 kW) and high (900 kW) power deposition (W/m^2) is shown in figure 1. The profile is very similar in the two cases as, in the experiment, we have designed the beam parameters on purpose to achieve comparable profiles at different powers.

B. Time trace of neutron emission measurements

Neutron emission is measured by the calibrated Scionix-EJ301A liquid scintillator used also in our previous experiment[12]. The scintillator measures the neutron counting rate and was coupled to an active base H10580 Hamamatsu photomultiplier tube (PMT). The detector was installed in vicinity of one of the two inner walls of the ELISE facility, at a distance of approximately 2.8 m behind the beam dump and with same experimental arrangement described in reference[12]. Signals coming from the detector were digitized by means of a 14 bit, 400 MS/s custom digitizer based on the ATCA platform[20,21]. A neutron low energy threshold of 1.15 MeV was used in the measurements. Neutron/gamma-ray discrimination is based on standard long/short gate charge integration. We estimate the probability of a wrong neutron/gamma-ray event discrimination to be about 6%. A neutron/gamma-ray ratio of about 3 was found experimentally.

III. LOCAL MIXING MODEL BASED CALCULATIONS

Neutron emission calculations are based on the LMM model of deuterium implantation in the dump, where diffusion or migration of deuterium is neglected once it is implanted. In more details, the flux of deuterium beam on the ith row and jth column block of the dump, at a depth z and at a time t, $\Phi_{i,j}(z,t)$, can be calculated as

$$\Phi_{i,j}(z,t) = \Phi_{i,j}(0,t)(1 - \int_0^z p(x)dx) \qquad (1)$$

Here $p(x)$ is the probability for the deposition of a deuteron at a depth x and depends on the incident energy significantly. In the LMM, no other reactions but deposition has been assumed and the probability of deposition in depth has been normalised to one. The TRansport of

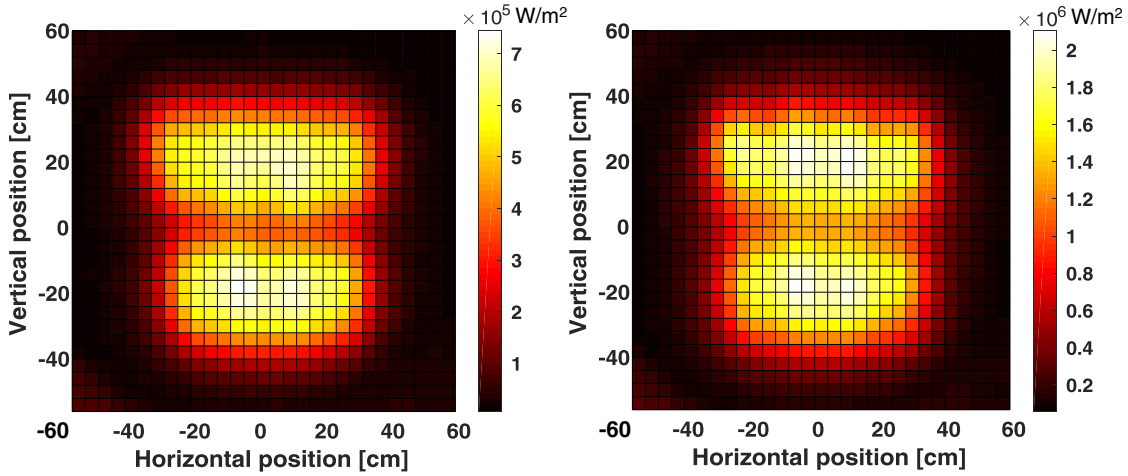

FIG. 1: Beam profile measured in the neutron emission experiment by the ELISE infra-red camera at low (300 kW, left) and high (900 kW, right) power deposition.

Ion in Matter (TRIM) code[22] has been applied to calculate the $p(x)$ for 27-60 keV incident deuterons with a step of 0.5 keV. The dump density was set to 8.902 g/cm^3. $\Phi_{i,j}(0,t)$ is the incident deuterium flux. This is in turn given by

$$\Phi_{i,j}(0,t) = \frac{I_{i,j}}{\Delta S \cdot q} \quad (2)$$

where $I_{i,j}$ is the current that reaches the ith row and jth column block of the dump, ΔS is the area of each block and q is the ion charge. $I_{i,j}$ is obtained by dividing the known power on each block by the acceleration voltage. The time resolved neutron yield from the dump $Y(t)$ can be determined from $\Phi_{i,j}(z,t)$ as

$$Y(t) = \sum_{i=1}^{30}\sum_{j=1}^{30}\int_0^R \Phi_{i,j}(z,t) n_{i,j}(z,t)\sigma(z,t)dz \times \Delta S \quad (3)$$

Here, $n_{i,j}(z,t)$ is the time dependent number of deuterons that get deposited per unit volume at a depth z, $\sigma(z,t)$ is the $D(d,n)^3He$ neutron production cross section (see below).

Ion implantation of hydrogen isotopes into metals can yield high concentrations of atoms[23]. The concentration here is defined as the percentage of deuterons to target atoms per unit volume. As the incident deuterons penetrate in the dump, the local deuteron concentration increases until a maximum is reached (saturation) and which depends on the target material[13]. Based on the results of our previous experiment[9,12], we have used 20% as concentration at saturation[24].

The cross section $\sigma(z,t)$ is related to the deuteron energy. The energies of deuterons at depth z have been calculated by using the total stopping power data from the TRIM code so to convert the energy dependent $D(d,n)^3He$ cross section to a function that depends on the depth z. Figure 2 shows an example of the deuteron energy and the $D(d,n)^3He$ cross section as a function of depth for 40 keV incident deuterons. From the figure we note that the effective layer from which neutrons are produced is only 0.5 μm thick and that most neutrons are produced within the first 0.2 μm.

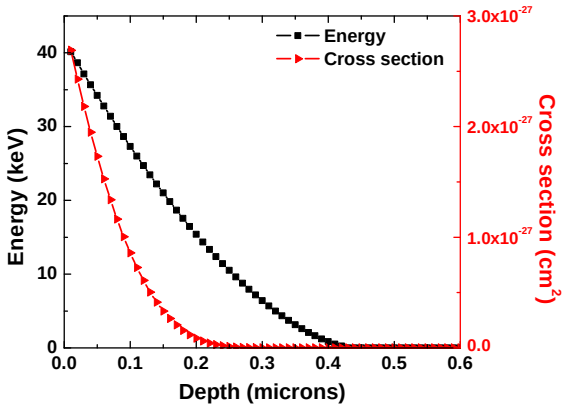

FIG. 2: Deuteron energy (left scale) and the $D(d,n)^3He$ cross section (right scale) as a function of depth at 40 keV

IV. RESULTS

Before the dedicated experiment, a set of experiments with a 22-44 keV deuterium beam was performed from the beginning of the deuterium campaign so that we could assume that deuterium density reached saturation before our dedicated investigation. Figure 3 shows the LMM based calculation of the time trace of neutron emission together with the measurement in our dedicated experiment. The calculation is based on equation 3 and uses as input the measured diagnostic information on the beam (current, voltage, profile). In general the LMM based calculation reproduces the basic features of the emission, i.e. the step ladder increase of the neutron yield as the beam power on the target is increased. In or-

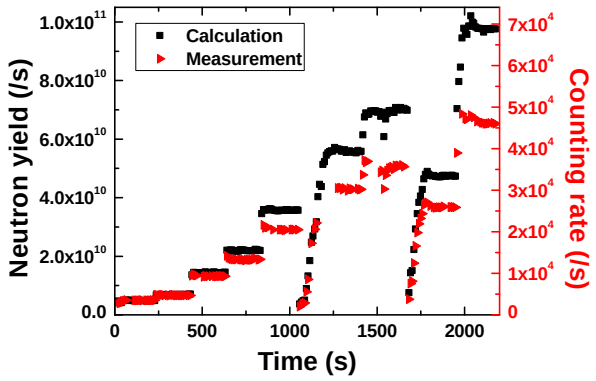

FIG. 3: Calculated neutron emission from the dump as a function of time (left axis) compared to the measured counting rate (right axis)

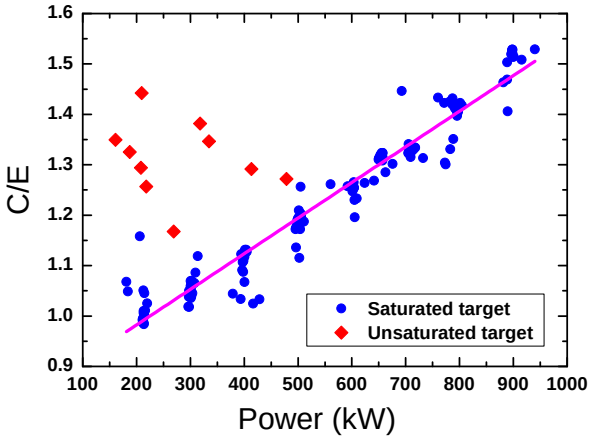

FIG. 5: Ratio C/E between the calculated and measured neutron emission as a function of the power on the dump

der to compare simulations and measurements in a more quantitative way the conversion coefficient k from $Y(t)$ (neutron/s from the target) to the detector counting rate must be determined. As k depends only on the neutron transport from the dump to the detector, it can be empirically evaluated by the ratio between the simulation and measurements at one experimental point where the LMM based calculation is assumed to be correct, and data at 200 kW on the dump between t=114 s and t=209 s have been used to calculate k.

Using this value, we can then compare measurements and calculations on a quantitative ground, albeit on a relative scale, as shown in figure 4. If the LMM model held exactly at any power on the dump, we would expect a ratio between the calculated and experimental neutron rate $C/E = 1$, but this contradicts the experimental data. Instead, we observe that the model calculates systematically more neutrons than found experimentally, i.e. $C/E > 1$. A graph of C/E as a function of the power on the dump (figure 5) shows a linear correlation between the two parameters, but for a few outliers. These correspond to the first few pulses of each experimental day when, presumably, a full saturation of the deuterium concentration in the dump was not yet reached. A linear fit to the data of figure 5 yields $C/E = (7.1 \pm 0.1) \times 10^{-4} \times Power + (0.841 \pm 0.008)$. The C/E values obtained by the experimental fit in this paper agree within 5% with those found in our previous study[15] in the lower power range where the two experiments overlap.

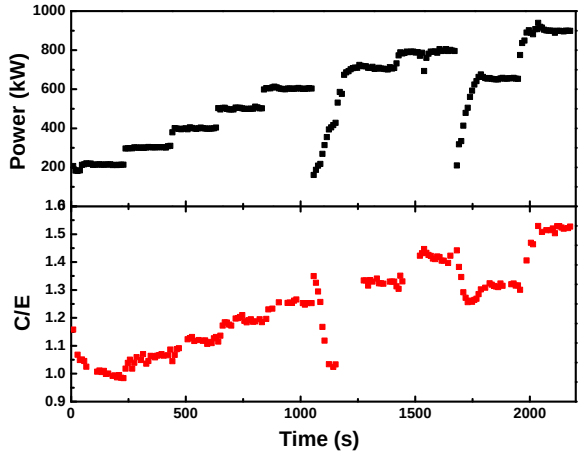

FIG. 4: (top) Beam power impinging on the dump as a function of time (bottom) Ratio between the calculated and measured neutron yield as a function of time

V. DISCUSSION

LMM based calculations require three measured quantities as input, i.e. the beam profile, current on the dump and the beam voltage. Each of them has an estimated uncertainty of 5%, which yields to an uncertainty in the calculation and is reflected in the fluctuation of the points at each constant power level in figure 5. Although this is certainly a visible effect, its magnitude is lower than the systematic trend of the deficit observed in the same figure and we judge it to have a negligible impact on our conclusion on the discrepancy between LMM based calculation and data.

In order to understand the results of figure 5 we can make the hypothesis that the dominant effect is a reduction of the deuterium concentration at saturation as a function of temperature. Qualitatively, one can expect temperature to promote the diffusion of deuterium in the dump and we here speculate that this is manifested in the different concentration reached at saturation as a function of temperature. The IR diagnostics installed at ELISE determines the difference ΔT between the average temperature of each individual block of the beam dump before and after irradiation[11]. By defining the hypothetical temperature dependent saturation rate (HTDSR) as the concentration at saturation required to exactly match the experimental data at each temperature, we can use the results of the experiment to find HTDSR as a function of ΔT averaged over the dump surface (figure 6). As for figure 3, we have assumed that the concentration at

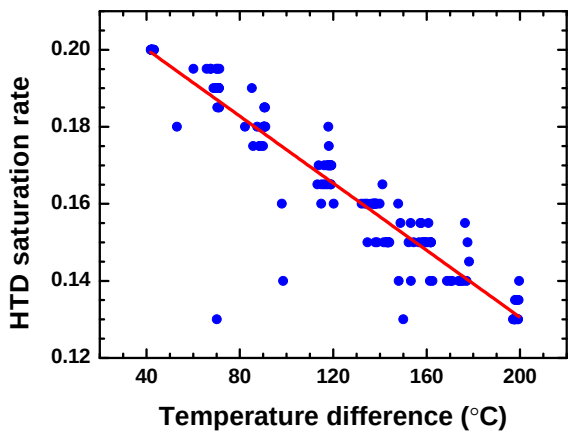

FIG. 6: Temperature dependent saturation rate as a function of the temperature difference after and before the beam irradiation.

saturation is 20% at a power of 200 kW. Data show a linear decrease of HTDSR versus ΔT which is described as $HTDSR = -4.35 \times 10^{-4} \times \Delta T + 0.218$. This formula can be used as an empirical correction for neutron emission calculations at SPIDER.

VI. CONCLUSIONS

A dedicated experiment on beam-target neutron emission has been performed at the ELISE neutral beam test facility to study the discrepancy between measurements and calculations in a power density range approaching that of SPIDER. The time trace of the neutron emission has been monitored by a calibrated neutron detector and the Local Mixing Model has been applied for predictions. The ratio between calculations and measurements (C/E) on a relative scale has been found to exceed unity beyond the observed fluctuation level of the data points at constant power and to scale linearly with the beam power in the range 200 kW to 950 kW. Assuming this can be explained by a temperature dependent saturation rate of deuterons in the target, an empirical correction to neutron emission calculations for applications at SPIDER has been derived.

VII. ACKNOWLEDGEMENTS

The work leading to this publication was funded partially by Fusion for Energy under the Contract No. F4E-RFXPMS A-WP-2017. The views and expression expressed herein do not necessarily reflect those of the Fusion for Energy and ITER organizations.

[1] V. Toigo, D. Boilson, T. Bonicelli, R. Piovan, M. Hanada, A. Chakraborty, G. Agarici, V. Antoni, U. Baruah, M. Bigi, *et al.*, Nuclear Fusion **55**, 083025 (2015).
[2] V. Toigo, R. Piovan, S. Dal Bello, E. Gaio, A. Luchetta, R. Pasqualotto, P. Zaccaria, M. Bigi, G. Chitarin, D. Marcuzzi, *et al.*, New Journal of Physics **19**, 085004 (2017).
[3] R. Pasqualotto, M. Agostini, M. Barbisan, M. Bernardi, M. Brombin, R. Cavazzana, G. Croci, M. D. Palma, R. Delogu, G. Gorini, *et al.*, in *AIP Conference Proceedings*, Vol. 1869 (AIP Publishing, 2017) p. 030020.
[4] F. Murtas, G. Croci, G. Claps, M. Cavenago, M. Dalla Palma, G. Gervasini, G. Grosso, R. Pasqualotto, E. P. Cippo, M. Rebai, *et al.*, in *Nuclear Science Symposium and Medical Imaging Conference (NSS/MIC), 2011 IEEE* (IEEE, 2011) pp. 405–408.
[5] G. Croci, M. Rebai, G. Claps, M. Cavenago, M. Dalla Palma, G. Gervasini, G. Grosso, F. Murtas, R. Pasqualotto, E. P. Cippo, *et al.*, Journal of Instrumentation **7**, C03010 (2012).
[6] A. Muraro, G. Croci, G. Albani, C. Cazzaniga, G. Claps, M. Cavenago, G. Grosso, M. Dalla Palma, M. Fincato, F. Murtas, *et al.*, Fusion Engineering and Design **96**, 311 (2015).
[7] A. Muraro, G. Croci, G. Albani, G. Claps, M. Cavenago, C. Cazzaniga, M. Dalla Palma, G. Grosso, F. Murtas, R. Pasqualotto, *et al.*, Nuclear Instruments and Methods in Physics Research Section A: Accelerators, Spectrometers, Detectors and Associated Equipment **813**, 147 (2016).
[8] M. Rebai, M. Cavenago, G. Croci, M. Dalla Palma, G. Gervasini, F. Ghezzi, G. Grosso, F. Murtas, R. Pasqualotto, E. Perelli Cippo, *et al.*, Review of Scientific Instruments **83**, 02B721 (2012).
[9] M. Rebai, PhD Thesis, http://hdl.handle.net/10281/28449 (2012).
[10] M. Rebai, G. Croci, G. Grosso, A. Muraro, E. P. Cippo, M. Tardocchi, M. Dalla Palma, R. Pasqualotto, M. Tollin, F. Murtas, *et al.*, Journal of Instrumentation **12**, C01007 (2017).
[11] R. Nocentini, F. Bonomo, A. Pimazzoni, U. Fantz, P. Franzen, M. Fröschle, B. Heinemann, R. Pasqualotto, R. Riedl, B. Ruf, *et al.*, in *AIP Conference Proceedings*, Vol. 1655 (AIP Publishing, 2015) p. 060006.
[12] X. Xufei, M. Nocente, F. Bonomo, P. Franzen, M. Fröschle, G. Grosso, F. Grünauer, R. Pasqualotto, M. Tardocchi, T. Fan, *et al.*, Review of Scientific Instruments **85**, 11D864 (2014).
[13] B. Doyle, D. Brice, and W. Wampler, Radiation Effects Letters **57**, 81 (1980).
[14] D. Brice, B. Doyle, and W. Wampler, Journal of Nuclear Materials **111**, 598 (1982).
[15] M. Nocente, S. Feng, D. Wünderlich, F. Bonomo, G. Croci, U. Fantz, B. Heinemann, W. Kraus, I. Mario, R. Pasqualotto, *et al.*, Fusion Engineering and Design **123**, 843 (2017).
[16] P. Franzen, U. Fantz, D. Wünderlich, B. Heinemann, R. Riedl, W. Kraus, M. Fröschle, B. Ruf, R. Nocentini, N. Team, *et al.*, Nuclear Fusion **55**, 053005 (2015).
[17] D. Wünderlich, U. Fantz, B. Heinemann, W. Kraus, R. Riedl, C. Wimmer, N. Team, *et al.*, Nuclear Fusion **56**, 106004 (2016).
[18] A. Pimazzoni, PhD Thesis, http://tesi.cab.unipd.it/46495/ (2014).
[19] R. Nocentini, U. Fantz, P. Franzen, M. Froeschle, B. Heinemann, R. Riedl, B. Ruf, D. Wuenderlich, *et al.*, Fusion Engineering and Design **88**, 913 (2013).
[20] M. Nocente, M. Tardocchi, I. Chugunov, R. Pereira, T. Edlington, A. Fernandes, D. Gin, G. Grosso, V. Kiptily, A. Murari, *et al.*, Review of scientific instruments **81**, 10D321 (2010).
[21] M. Nocente, M. Tardocchi, A. Olariu, S. Olariu, R. Pereira, I. Chugunov, A. Fernandes, D. Gin, G. Grosso, V. Kiptily, *et al.*, IEEE Transactions on Nuclear Science **60**, 1408 (2013).
[22] J. F. Ziegler, M. D. Ziegler, and J. P. Biersack, Nuclear Instruments and Methods in Physics Research Section B: Beam Interactions with Materials and Atoms **268**, 1818 (2010).
[23] W. Möller, Nuclear Instruments and Methods in Physics Research **209**, 773 (1983).
[24] J. Kim, Nuclear Technology **44**, 315 (1979).